Scissored-Pair Control Moment Gyros: A Mechanical Constraint Saves Power

Daniel Brown[1] and Mason A. Peck[2]
Cornell University, Ithaca, New York, 14853

Introduction

SCISSORED-pair control-moment gyros have been around for over a century. Brennan's monorail used two counter-rotating flywheels with gearing between their gimbals to provide symmetric stabilization around left or right turns [1, 2]. Also referred to as twin gyros, scissored pairs maintain equal-magnitude and opposite-sign gimbal angles for two control-moment gyros (CMGs) with parallel gimbal axes [3, 4]. A scissored pair, like any array of CMGs, provides attitude-control torque via momentum exchange with the body on which it is mounted. The Skylab-era Astronaut Maneuvering Research Vehicle used scissored pairs for attitude control [5, 6]. These devices have also been studied as gyrodampers of large space structures [7, 8]. A robot with single revolute joints requires output torque along a single axis. The enforced symmetry of a scissored pair provides such a torque without introducing large reaction torques in the robot. Such a system could be used to rapidly maneuver a payload with less power than rapidly maneuvering the entire spacecraft [9].

We consider a scissored pair that uses a mechanical constraint, such as gears or a mechanical linkage, to enforce the gimbal symmetry. We compare it to a scissored pair of independent CMGs. Each CMG in a scissored pair of independently driven CMGs has its own gimbal motor, which needlessly uses power to react what should be a workless constraint torque. As explained in this note, the gear cancels certain torques that would otherwise act on the independent CMGs. The gear also replaces the two independent gimbal motors with a single motor, which may represent improved mass and volume efficiency in the electromechanical design. An early double-gimbal CMG concept with mechanical synchronization is described by Liska [10]. This note discusses the reduction in power use and the effect on motor size that a geared scissored pair provides as compared to an independent scissored pair.

Scissored pairs attempt to mitigate some of the difficulties associated with traditional CMGs that arise from the changing direction of the CMG output torque. Accommodating the changing output-torque direction is among the greatest challenges of CMG-based attitude-control system design because this effect can lead to internal singularities

---

[1] Graduate Student, Mechanical Engineering, 138 Upson, Student Member AIAA.
[2] Assistant Professor, Sibley School of Mechanical and Aerospace Engineering, 212 Upson, Member AIAA.
This paper appears in Journal of Guidance, Control, and Dynamics, vol. 31, No. 6, pp. 1823-1826, 2008

[11]. When a CMG array is singular, it cannot produce the commanded torque. Singularities in scissored pairs occur only if the commanded torque exceeds the capability of the scissored pair in magnitude or if the momentum stored in the pair is at a maximum. These saturation singularities occur in any actuator. Scissored pairs otherwise offer a singularity-free range of angular momentum, unlike other CMG array geometries [12]. Essentially a scissored pair array provides a set of constant-direction, variable-magnitude momentum vectors whereas typical CMG arrays provide a set of constant-magnitude, variable-direction momentum vectors. Scissored pairs also have a unique zero-angular-momentum configuration, which simplifies maneuver design. However, their singularity-free performance artificially limits the momentum envelope of a scissored-pair array by constraining the available output torque of the pair to a single line instead of a disc. This note does not investigate the relative merits of such an array. Rather, we focus on the internal torque cancellation and the resulting power savings for a geared scissored pair as compared to an independent scissored pair.

Analysis

In this analysis, the combined inertia dyadic of the gimbal structure and the rotor $\boldsymbol{I}_{gr}$ of each CMG is assumed to be spherical and hence constant in any frame. Using $\boldsymbol{1}$ to represent the unit dyadic, the CMG inertia is expressed as:

$$\boldsymbol{I}_g + \boldsymbol{I}_r = \boldsymbol{I}_{gr} = I_{gr}\boldsymbol{1} \tag{1}$$

The gimbal torque errors due to this assumption are small, as discussed below. This value also incorporates the effective inertia due to output-axis compliance [13]. The gimbal angle, ϕ, the body rate relative to the inertial N frame, $\boldsymbol{\omega}^{\mathrm{B/N}}$, and the rotor momentum, $\mathbf{h}_r$, which is constant in the gimbal frame, are shown in Fig. 1. The gimbal axis, $\hat{\boldsymbol{g}}$, comes out of the page. Taking the derivative in the gimbal frame and applying the transport theorem gives the derivative of the CMG angular momentum:

$$\overset{\mathrm{N}}{\boldsymbol{h}}_c = I_{gr} \cdot \left(\ddot{\phi}\hat{\boldsymbol{g}} + \overset{\mathrm{B}}{\boldsymbol{\omega}}{}^{\mathrm{B/N}} - \dot{\phi}\hat{\boldsymbol{g}} \times \boldsymbol{\omega}^{\mathrm{B/N}} \right) + \left(\dot{\phi}\hat{\boldsymbol{g}} + \boldsymbol{\omega}^{\mathrm{B/N}} \right) \times \boldsymbol{h}_r \tag{2}$$

An overdot indicates the time derivative of a scalar, and we use the following notation to indicate a derivative in the N frame:

$$\frac{{}^{\mathrm{N}}d}{dt}\boldsymbol{h} = \overset{\mathrm{N}}{\boldsymbol{h}} \tag{3}$$

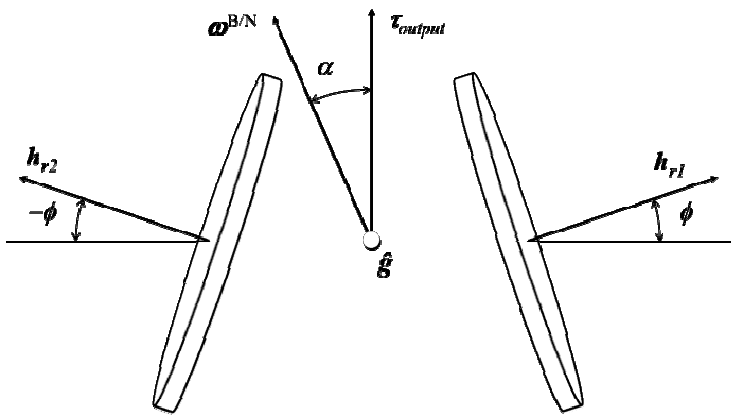

Fig. 1 Scissored pair geometry.

The torque applied by the gimbal motor on the first of the two CMGs acts only along the gimbal axis and is the dot product of $\hat{\mathbf{g}}$ and Eq. (2). For the second CMG of the scissored pair, the gimbal rate is opposite the first. The rotor momentum magnitude is identical for each CMG, but the direction is not. Therefore, $\boldsymbol{h}_{r1} \neq \boldsymbol{h}_{r2}$. We construct a control volume for each gimbal to isolate the individual gimbal torques as shown in Fig. 2. Another control volume including only the single motor for the scissored pair and each of the gimbal torques shows that a gear results in a net applied torque, τ_A, equal to the difference between the two gimbal torques.

$$\tau_{g1} = I_{gr}\ddot{\phi} + I_{gr}\,{}^{B}\dot{\boldsymbol{\omega}}^{B/N} \cdot \hat{\boldsymbol{g}} + \left(\boldsymbol{\omega}^{B/N} \times \boldsymbol{h}_{r1}\right) \cdot \hat{\boldsymbol{g}} \tag{4}$$

$$\tau_{g2} = -I_{gr}\ddot{\phi} + I_{gr}\,{}^{B}\dot{\boldsymbol{\omega}}^{B/N} \cdot \hat{\boldsymbol{g}} + \left(\boldsymbol{\omega}^{B/N} \times \boldsymbol{h}_{r2}\right) \cdot \hat{\boldsymbol{g}} \tag{5}$$

$$\begin{aligned} \tau_A &= \tau_{g1} - \tau_{g2} \\ &= 2I_{gr}\ddot{\phi} + \left[\boldsymbol{\omega}^{B/N} \times \left(\boldsymbol{h}_{r1} - \boldsymbol{h}_{r2}\right)\right] \cdot \hat{\boldsymbol{g}} \end{aligned} \tag{6}$$

We neglect the obvious disadvantage of friction and backlash in the gears, but also note that gears could reduce or eliminate misalignment of the gimbal angles [14].

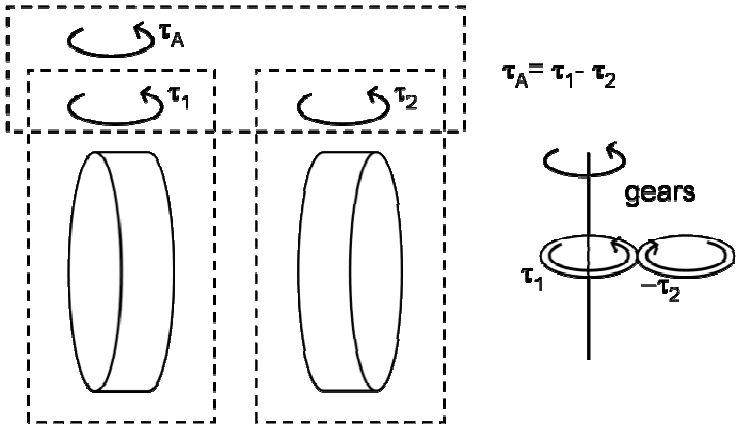

Fig. 2 Total torque and gimbal torques for a geared scissored pair.

The mechanical power used by the CMGs for a maneuver is the product of gimbal torque and rate.

$$\left|P\right| = \left|\tau_g \dot{\phi}\right| \tag{7}$$

Both positive and negative power are assumed to require energy from the spacecraft power subsystem. Therefore we consider the absolute value of power in our comparisons. The sign would matter in a case where the spacecraft power system efficiently recovered this energy expenditure in a regenerative fashion, e.g. using the gimbal motor as a generator. We assume that such an architecture is not in place for purposes of this study. Here, power is independent of the sign of gimbal torque and gimbal rate. For a lossless system that perfectly returns negative power to the system, there is no distinction between geared and independent scissored pairs.

The rotor-momentum terms typically dominate the product-of-inertia terms in Eqs. (4) to (6), justifying the CMG inertia in Eq. $\boldsymbol{I}_g + \boldsymbol{I}_r = \boldsymbol{I}_{gr} = I_{gr}\boldsymbol{1}$ (1) and providing the following approximation for the gimbal torque:

$$\tau_{gi} \approx \left(\boldsymbol{\omega}^{\mathrm{B/N}} \times \boldsymbol{h}_{ri}\right) \cdot \hat{\boldsymbol{g}} \tag{8}$$

The body rate largely determines CMG power use because of this base-rate effect on gimbal torque. Geared scissored pairs can reduce base-rate effects through internal torque cancellation. This result neglects losses due to friction and electromagnetic inefficiencies under the likely assumption that the gimbal torque *per se* drives the power design in an agile application. Such losses may make CMGs an inefficient choice for a generally quiescent robotic system.

From this result, the approximate power for the geared or the independent scissored pair is

$$P_{geared} \approx \left| \left[\boldsymbol{\omega}^{\mathrm{B/N}} \times \left(\boldsymbol{h}_{r,1} - \boldsymbol{h}_{r,2} \right) \right] \cdot \hat{\boldsymbol{g}} \right| \left| \dot{\phi} \right| \tag{9}$$

$$P_{independent} \approx \left| \left(\boldsymbol{\omega}^{\mathrm{B/N}} \times \boldsymbol{h}_{r,1} \right) \cdot \hat{\boldsymbol{g}} \right| \cdot \left| \dot{\phi} \right| + \left| \left(\boldsymbol{\omega}^{\mathrm{B/N}} \times \boldsymbol{h}_{r,2} \right) \cdot \hat{\boldsymbol{g}} \right| \cdot \left| \dot{\phi} \right| \tag{10}$$

The portion of $\boldsymbol{\omega}^{\mathrm{B/N}}$ along the gimbal axis does not affect this result. Therefore, we consider only the projection of body rate onto the plane normal to $\hat{\boldsymbol{g}}$. This projection is represented as a magnitude, $\|\boldsymbol{\omega}\|$, and an angle, α, at which the rate is oriented relative to the output axis of the scissored pair, as shown in Fig. 1. The magnitude of the body rate, rotor momentum, and gimbal rate can be factored out of Eqs. (9) and (10) to define a nondimensional power P^*:

$$P^* = P \Big/ \left(\|\boldsymbol{\omega}\| h_r \right) \tag{11}$$

$$P^*_{geared} \approx \left| 2 \cos\alpha \cos\phi \right| \tag{12}$$

$$P^*_{independent} \approx \left| \cos\left(\alpha - \phi\right) \right| + \left| \cos\left(\alpha + \phi\right) \right| \tag{13}$$

The nondimensional power of independent and geared scissored pairs is shown for one quadrant of the gimbal-angle, body-rate-angle space in Fig. 3a&b. Symmetry of P^* about ϕ and α equal to $n \cdot \pi/2$ is apparent from Eqs. (12) and (13). (P^* repeats every $n \cdot \pi$.) The product $\|\boldsymbol{\omega}\| \cdot h_r$ is the same for every point on each surface so that an independent scissored pair can be compared to a geared pair. This result is relevant if considered over many maneuvers, in which the gimbal rate and body rate are uniformly distributed over the body-rate and gimbal angles. At the origin the power is at a peak, as expected, because the scissored pair is directly responsible for the work done on the body. When the scissored pair saturates and the body rate is perpendicular to the output axis (ϕ and α each approach $\pm\pi/2$), the opposing torques add for the independent scissored pair but are canceled internally for the geared scissored pair. In the quadrant shown, the geared scissored pair offers a clear advantage over the independent scissored pair for $\alpha+\phi>\pi/2$. For $\alpha+\phi<\pi/2$, the two require the same power. The peak torque and power of the motor on the geared scissored pair is theoretically twice that of the independent scissored pair. However, if no momentum bias exists in the spacecraft system, then the body rate is zero when all gimbal angles in an array are zero. In this likely case, the geared scissored pair has a lower peak power at the origin while the independent scissored pair must still account for the second peak in power at $(\phi,\alpha)=(\pi/2,\pi/2)$.

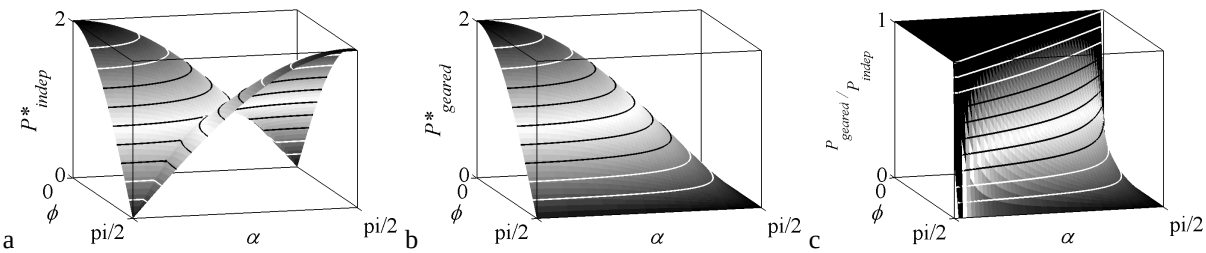

Fig. 3 Nondimensional power of scissored pairs. a) *Independent scissored pair.* **b)** *Geared scissored pair.* **c)** *Power ratio.*

The ratio of power for the geared scissored pair to power for the independent scissored pair as a function of ϕ and α is found from Eqs. (12) and (13). The body-rate magnitude, rotor momentum, and gimbal rate divide out.

$$\frac{P_{geared}}{P_{independent}} \approx \frac{\left|2\cos\alpha\cos\phi\right|}{\left|\cos\left(\alpha-\phi\right)\right|+\left|\cos\left(\alpha+\phi\right)\right|} \tag{14}$$

This ratio is shown in Fig. 3c as a function of base-rate angle α and gimbal angle ϕ. The volume of the region where the ratio is less than one represents the power savings. The volume enclosed by the surfaces in Fig. 3a&b represents simplistically the total power over many maneuvers with uniformly distributed body and gimbal angles and rates. The ratio of the total enclosed volumes, found by integrating Eqs. (12) and (13), is $2/\pi$. These results do not show the contribution of output-axis compliance, which adds an offset to Fig. 3, dependent on the particular CMG design. These results can be used to optimize the design of a CMG array and maneuver planning for power usage, and therefore agility, of a spacecraft controlled by scissored pairs. Other design considerations, e.g., total mass, motor size, fault tolerance, and system complexity, are also likely impacted by this strategy but are not discussed here.

For a spacecraft with three rotational degrees of freedom, an array of three orthogonal scissored pairs provides a cube-shaped singularity-free region with sides of length $4\cdot h_r$. We use this array architecture to illustrate the possible advantages afforded by a geared scissored pair. The maximum angular momentum is $4\sqrt{3}\cdot h_r$ at the cube's corners. The gimbal angles for a given spacecraft momentum are easily found by projecting the spacecraft momentum vector onto the output axis of each scissored pair. Likewise, the body-rate angle α is the arccosine of the dot product of the body-rate unit vector and the output axis of the scissored pair. For a spacecraft with spherical inertia, the body rate is proportional to the spacecraft momentum. In this case, the geared and independent scissored pairs are equivalent when the array momentum lies within a momentum sphere of radius $2\cdot h_r$. The geared scissored pairs outperform their counterparts near the corners of the momentum envelope. For a time-optimal maneuver with actuator saturation

[15] this region would be well used and represents 48% of the total momentum volume. Abrupt changes in attitude before the spacecraft comes to rest would further increase α and ϕ in favor of the geared scissored pairs. This comparison considers only two types of scissored-pair arrays. The added power cost for the independent scissored pair array is due to an enforced null motion [16, 17], indicating that not all null motions are created equal.

Simulations

We simulate the agile spacecraft described in Ref. [18] for a simple rotation about an axis. Three orthogonal scissored pairs provide actuation. The spacecraft angle, rate, and acceleration with finite jerk for a 30 degree maneuver are shown in Fig. 4. The peak rate is 6 degrees per second [18]. We calculate the CMG momentum as

$$|2\boldsymbol{h}_r|=|\boldsymbol{I}_s\boldsymbol{\omega}^{\mathrm{B/N}}| \tag{15}$$

The CMG momentum is 0.1314 kg·m^2/s. To utilize the corners of the momentum cube, the peak body rate is scaled by √3 for those maneuvers. The spacecraft inertia is 2.5·$\boldsymbol{1}$ kg·m^2. The scissored pair's output axes align with the spacecraft frame basis vectors.

The spacecraft rotates smoothly about the [1 0 0] (face normal) or the [1 1 1]/√3 (corner) axis to represent the range of loads on the scissored pairs when operating on the momentum envelope. The maximum gimbal angle is 85 degrees. We calculate the peak torque and power of any single gimbal motor in the array, the peak power of the entire array, and the total energy used for the maneuver. The results are summarized in Table 1. The independent scissored pairs have the greatest peak torque because they must work against the base-rate effect while doing little work on the spacecraft; i.e. the scissored pair constraint enforces a costly null motion. The geared scissored pair has a higher peak power by only 20% over the independent scissored pair because of internal torque cancelations, indicating that one motor with gearing reduces mass over two independent gimbal motors in a scissored pair. The spacecraft power subsystem can also be smaller for the geared scissored pair since the peak power is 36% less than for the independent scissored pair. As expected from the analysis, the geared and independent scissored pair arrays use the same amount of energy when operating on a face of the momentum cube, but the geared scissored pairs use less energy at the corners. The body rate effect causes the peak gimbal power of the geared scissored pair to be less at the faster corner maneuver than the face maneuver even though peak torque is the same.

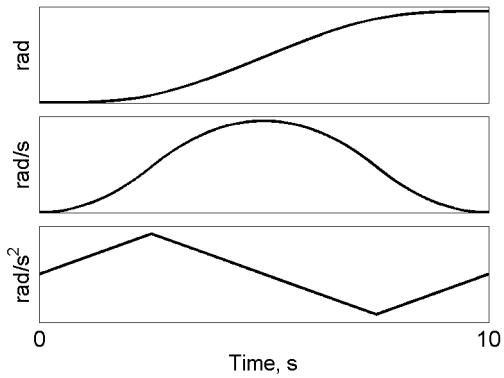

Fig. 4 Commanded spacecraft angle, rate, and acceleration.

Table 1 Peak torque and power for geared and independent scissored pairs.

Location on momentum cube	Peak body rate, rad/s	Peak torque per motor, mN·m		Peak power per motor, mW		Peak total power, mW		Total energy, mJ	
		Gear	Indep.	Gear	Indep.	Gear	Indep.	Gear	Indep.
Face center	0.1049	13.9	7.0	6.0	3.0	6.0	6.0	27.5	27.5
Corner	0.1816	14.0	16.8	4.5	5.0	13.6	21.4	82.5	129

Conclusions

A seemingly inconsequential use of a mechanical constraint between the CMGs of a scissored pair provides internal torque cancellation when otherwise the power used would increase. This advantage occurs near the limit of the scissored pair's momentum capacity, a vital region for maximizing performance. A small satellite attitude control system illustrates the effects of the internal torque cancellation provided by a mechanical constraint on peak torque, power, and energy used. A geared scissored pair may reduce the overall mass of the scissored pair by replacing two motors, and the extra housing, harness, and connector mass, with one motor and the connecting gears. Non-linearities in the gears or mechanism connecting the CMGs may affect these results; thus actual power savings would depend on the hardware implementation. The independent scissored pair performs poorly relative to the geared scissored pair in simulations because they perform costly null motions that are affected by the base rate. The base rate effects are cancelled internally via the mechanical coupling. This conclusion may have implications for mull motions of arbitrary CMG arrays, although such concerns are not investigated in this note.

Acknowledgments

D. Brown was supported by an NSF Integrative Graduate Education and Research Traineeship (IGERT) grant.

References

[1] Brennan, L., "Improvements in and Relating to the Imparting of Stability to otherwise Unstable Bodies, Structures or Vehicles," GB Patent 27,212, 1903,

[2] Brennan, L., "Means for Imparting Stability to Unstable Bodies," US Patent 796893, 1905,

[3] Crenshaw, J.W., "2-SPEED, A Single-Gimbal Control Moment Gyro Attitude Control System," *AIAA Guidance and Control Conference,* AIAA, Washington, DC, 1973, pp. CP895.

[4] Havill, J.R., and Ratcliff, J.W., "A Twin-Gyro Attitude Control System for Space Vehicles," *NASA TN D-2419,* 1964,

[5] Cunningham, D.C., and Driskill, G.W., "A Torque Balance Control Moment Gyroscope Assembly for Astronaut Maneuvering," *NASA Ames Research Center 6th Aerospace Mechanisms Symposium,* 1972, pp. 121-126.

[6] Murtagh, T.B., Whitsett, C.E., Goodwin, M.A., "Automatic Control of the Skylab Astronaut Maneuvering Research Vehicle," *Journal of Spacecraft and Rockets,* Vol. 11, No. 5, 1974, pp. 321-326.

[7] Yang, L.F., Mikulas, M.M., Jr, Park, K.C., "Slewing Maneuvers and Vibration Control of Space Structures by Feedforward/Feedback Moment-Gyro Controls," *Journal of Dynamic Systems, Measurement, and Control,* Vol. 117, 1995, pp. 343-351.

[8] Aubrun, J.N., and Margulies, G., "Gyrodampers for Large Space Structures," NASA, 159171, 1979.

[9] Carpenter, M.D., and Peck, M.A., "Dynamics of a High-Agility, Low-Power Imaging Payload," *IEEE Transactions on Robotics,* 2008 (To appear),

[10] Liska, D., "A Two-Degree-of-Freedom Control Moment Gyro for High-Accuracy Attitude Control," *Journal of Spacecraft and Rockets,* Vol. 5, No. 1, 1968, pp. 74-83.

[11] Kurokawa, H., "Survey of Theory and Steering Laws of Single-Gimbal Control Moment Gyros," *Journal of Guidance, Control, and Dynamics,* Vol. 30, No. 5, 2007,

[12] Elgersma, M.R., Johnson, D.P., Peck, M.A., "Method and System for Controlling Sets of Collinear Control Moment Gyroscopes," US Patent Application A1 20070124032, 2007,

[13] Liden, S.P., "Precision CMG Control for High-Accuracy Pointing," *Journal of Spacecraft and Rockets,* Vol. 11, 1974, pp. 236.

[14] Yang, L.F., and Chang, W.H., "Synchronization of Twin-Gyro Precession Under Cross-Coupled Adaptive Feedforward Control," *Journal of Guidance, Control, and Dynamics,* Vol. 19, No. 3, 1996, pp. 534-539.

[15] Wie, B., Bailey, D., and Heiberg, C., "Rapid Multitarget Acquisition and Pointing Control of Agile Spacecraft," *Journal of Guidance, Control, and Dynamics,* Vol. 25, No. 1, 2002, pp. 96-104.

[16] Bedrossian, N.S., Paradiso, J., Bergmann, E.V., "Steering Law Design for Redundant Single-Gimbal Control Moment Gyroscopes," *Journal of Guidance, Control, and Dynamics,* Vol. 13, No. 6, 1990, pp. 1083–1089.

[17] Vadali, S.R., Walker, S.R., and Oh, H.S., "Preferred Gimbal Angles for Single Gimbal Control Moment Gyros," *Journal of Guidance, Control, and Dynamics,* Vol. 13, 1990, pp. 1090-1095.

[18] Lappas, V.J., Steyn, W.H., and Underwood, C.I., "Attitude Control for Small Satellites Using Control Moment Gyros," *Acta Astronautica,* Vol. 51, No. 1-9, 2002, pp. 101-111.